Applied Catalysis A: General 498 (2015) 185–191

Contents lists available at ScienceDirect

Applied Catalysis A: General

journal homepage: www.elsevier.com/locate/apcata

Duality in the *Escherichia coli* and methicillin resistant *Staphylococcus aureus* reduction mechanism under actinic light on innovative co-sputtered surfaces

S. Rtimi[a], M.K.S. Ballo[a,b], D. Laub[c], C. Pulgarin[a], J.M. Entenza[b], A. Bizzini[b,d], R. Sanjines[e], J. Kiwi[a,*]

[a] Ecole Polytechnique Fédéral de Lausanne, EPFL-SB-ISIC-GPAO, Station 6, CH-1015 Lausanne, Switzerland
[b] Department of Fundamental Microbiology, University of Lausanne, CH-1015 Lausanne, Switzerland
[c] Ecole Polytechnique Fédéral de Lausanne, EPFL-SB-CIME-MXC 039, Station 12, CH-1015 Lausanne, Switzerland
[d] Department of Infectious Diseases, University Hospital Center, Lausanne (CHUV), Switzerland
[e] Ecole Polytechnique Fédérale de Lausanne, EPFL-SB-IPMC-LNNME, Bat PH, Station 3, CH-1015 Lausanne, Switzerland

ARTICLE INFO

Article history:
Received 17 January 2015
Received in revised form 19 March 2015
Accepted 24 March 2015
Available online 1 April 2015

Keywords:
Co-sputtered surfaces
TiO_2/Cu-PES
MRSA
E. coli
Bacterial reduction
Oligodynamic effect

ABSTRACT

The kinetics of bacterial reduction of *Staphylococcus aureus* (MRSA) on co-sputtered TiO_2/Cu-polyester (TiO_2/Cu-PES) was found to be little dependent on the applied light dose. But in the case of *Escherichia coli*, the bacterial reduction kinetics was observed to be strongly dependent on the applied light dose. The reasons for the different effect of the applied light dose on the bacterial reduction are discussed. Mechanistic considerations are suggested to account for this observation. TiO_2/Cu-PES obtained by direct current magnetron co-sputtering and the bacterial reduction features compared to PES sputtered individually by TiO_2 and Cu. This study presents the first evidence for the stabilizing effect of TiO_2 on the amounts of the Cu released during bacterial inactivation by co-sputtered surfaces compared to sequential sputtering of Ti and/or Cu on PES. The release of Cu-monitored in the ppb range by inductively coupled plasma-mass spectrometry (ICP-MS) is indicative of an oligodynamic effect leading to bacterial reduction. The bacterial reduction of MRSA ATCC 43300 on co-sputtered TiO_2/Cu led to a 5 $\log_{10}$ (99.999%) reduction within 120 min in the dark and 60 min under low intensity actinic light. Diffuse reflectance spectroscopy (DRS), transmission electron microscopy (TEM) and X-ray fluorescence (XRF) describe the TiO_2/Cu surfaces investigated in this study.

1. Introduction

Nanoparticulate films preparation able to kill pathogenic bacteria avoiding the formation of biofilms is a topic of increasing attention. Infections caused by antibiotic-resistant bacteria and leading to healthcare associated infections (HCAIs) with higher cost treatments [1–4]. Also, these nosocomial infections caused by antibiotic resistant bacteria are becoming more frequent [5]. Recently, some laboratories [6–9], have reported antibacterial Ag, Cu and TiO_2 coatings on glass and polymer films depositing the metal/oxides by chemical vapour deposition (CVD) and sputtering techniques. Direct current (DC) magnetron sputtering as used in this work allows the deposition of metal/metal oxides at relatively low temperatures not exceeding 120–130 °C which allow the sputtering on textiles and polymers presenting a low thermal resistance. Advances in bactericidal surfaces have become a focus of attention over the last five years. Studies on the photo-activated TiO_2 and Cu–TiO_2 mediated bacterial reduction have been reported [10–12]. There is a need for active, uniform and adhesive surfaces to decrease more effectively environmental risks associated with HAI.

Recent studies [13,14] have reported the preparation of Cu and TiO_2/Cu films by sol–gel methods inducing significant bacterial inactivation under UV–vis light. Nevertheless, the sol–gel preparations deposited films are not mechanically stable, nor reproducible, present low uniformity and little adhesion since they can be wiped off by a cloth or thumb [15]. This moved us to work on the preparation of sputtered antibacterial films to overcome the shortcomings of colloidal loaded films and motivated the present study.

Reduction of *Escherichia coli* on Cu-sputtered polyester (Cu-PES) [16,17] and reduction of MRSA on Cu-PES has recently been reported by our laboratory [18] and other sources [19]. This

* Corresponding author. Tel.: +41 21 6936150; fax: +41 21 6935690.
E-mail address: john.kiwi@epfl.ch (J. Kiwi).

http://dx.doi.org/10.1016/j.apcata.2015.03.028
0926-860X/

study is a continuation of our previous work on TiO_2/Cu surfaces leading to *E. coli* [17–19] reduction, but extending the previous studies to show: (a) the bacterial reduction on innovative TiO_2/Cu co-sputtered PES, (b) the differential effect of the applied actinic/visible light (400–700 nm) on the bacterial reduction kinetics of *E. coli* and MRSA and suggest the rationale for this, (c) the stabilizing effect of TiO_2 on the Cu release from the co-sputtered surfaces during bacterial reduction compared to Cu sputtered individually, (d) by inductively coupled plasma mass spectrometry (ICPMS) account for the Cu-oligodynamic effect leading to the observed bacterial reduction and (e) the effect of a co-sputtered catalyst TiO_2/Cu-PES on the bacterial reduction kinetics of Gram+ and Gram− bacteria, as well as the effect of actinic/visible intensity on the bacterial reduction on these two bacterial probes.

2. Experimental

2.1. Catalyst preparation

The PES used corresponds to the EMPA test cloth sample No 407. It is a polyester Dacron polyethylene terephthalate, type 54 spun, 130 microns thick, plain weave ISO 105-F04. Direct current magnetron sputtering deposition of Ti and Cu was carried out in a CMS-18 Vacuum system from Kurt Lesker Ltd. evacuated to 5.8×10^{-3} mbar by a turbo-molecular pump. The Cu as well as the Ti target were 2 inches in diameter, 99.99% pure from K. Lesker Ltd., UK. Co-sputtering was carried out at 300 mA and 350 V. The Ti and Cu targets used for the co-sputtering were positioned at 10 cm of the PES substrate. The nominal calibration of the film thickness was carried out on the Si-wafers and the film thickness was determined with a profilometer (Alphastep500, TENCOR).

2.2. Catalyst characterization

2.2.1. Surface loading

The X-ray fluorescence (XRF) determination of the Ti and Cu on PES was evaluated in a PANalytical PW2400 spectrometer.

2.2.2. Surface release during bacterial inactivation

A Finnigan™ ICP-MS (Inductively Coupled Plasma-Mass Spectrometry) was used to determine the Ti and Cu release during the bactericidal cycles with a resolution of 1.2×10^5 cps/ppb and detection limit of 0.2 ng/L. A washing solution of the TiO_2/Cu sample were digested with nitric acid 69% (1:1 $HNO_3 + H_2O$) to remove the organics in the solution and to guarantee that there were no remaining ions adhered to the flacon wall. The samples droplets are introduced to the ICP-MS trough a peristaltic pump to the nebulizer chamber at ~7700 °C allowing the evaporation and ionization of the elements in the sample. The Cu and Ti found in the nebulizer droplets were subsequently quantified by mass spectrometry.

2.2.3. Diffuse reflectance spectroscopy (DRS)

Diffuse reflectance spectroscopy (DRS) was carried out in a Perkin Elmer Lambda 900 UV–vis-NIR spectrometer within the wavelength range of 200–800 nm. The rough UV–vis reflectance data cannot be used directly to assess the absorption of the TiO_2/Cu/CuO-PES samples because of the large scattering contribution of the PES fabric to the DRS spectra. Normally a weak dependence is assumed for the scattering coefficient S on the wavelength. The spectra were plotted in Kubelka-Munk (KM) units.

2.2.4. High-resolution transmission electron microscopy (HRTEM) and stereomicroscopy

The transmission electron microscopy (TEM) required the PES fabrics embedding in epoxy resin (Embed 812) and cross-sectioned with an ultra-microtome (Ultracut E) up to a thin 2.25: Fluorescence stereomicroscopy and X-ray-photoelectron spectroscopy (XPS):

The fluorescence stereomicroscopy was carried out on samples inoculated with 10^8 CFU of *E. coli* and incubated for 2 h in a humidification chamber. This method uses a fluorochrome-based staining procedure from Filmtracer™ LIVE/DEAD® Biofilm Viability Kit (Molecular Probes, Invitrogen). The kit contains a combination of the SYTO 9® green fluorescent nucleic acid stain and propidium iodide fluoro-chromes for the staining of live and dead cells, respectively. The sample fluorescence was monitored in a fluorescence stereomicroscope (Leica MZ16 FA, Leica Microsystems GmbH Wetzlar, Germany) and the images were processed using the LAS v.1.7.0 build 1240 software from Leica Microsystems CMS GmbH. Adhesion of bacteria to the sputtered PES was allowed for 2 min before washing the sample with sterile Milli-Q water to remove non-adherent bacteria.

2.2.5. X-ray photoelectron spectroscopy of samples

The XPS of the samples was carried out in an AXIS NOVA unit (Kratos Analytical, Manchester, UK) equipped with monochromatic AlK_α ($h\nu$ = 1486.6 eV) anode and the deconvolution software CasaXPS-Vision 2. The carbon C1s line with position at 284.6 eV was used as a reference to correct the charging effects. The surface atomic concentration of some elements was determined from the peak areas and known sensitivity factors [20,21]. Spectrum background was subtracted using the program of the Kratos unit. The etching depth induced by the Ar-ions was referenced to the etching of Ta of 15 atomic layers per minute equivalent to ~3 nm/min.

2.3. Catalytic tests

2.3.1. Bacterial reduction and irradiation sources

Unsputtered and sputtered PES samples were sterilized in 70% ethanol and dried overnight at room temperature (RT). Cultures for the preparation of the MRSA ATCC 43300 and *E. coli* K12 inoculum were prepared by picking a single bacteria colony from the agar plate and incubated in tryptic soy broth at 37 °C overnight. Overnight cultures of the microorganisms were washed two times in 0.9% NaCl and lately diluted to the selected concentration.

E. coli K12 strains was obtained from the Deutsche Sammlung von Mikroorganismen und Zellkulturen GmbH (DSMZ) ATCC23716, Braunschweig, Germany, to test the antibacterial activity of the co-sputtered samples. The PES fabrics were sterilized by autoclaving at 121 °C for 2 h. The 20 μL culture aliquots with an initial concentration of ~10^6 CFU mL^{-1} in NaCl/KCl (pH 7) were placed on coated and uncoated (control) PES fabric. Samples were then placed on Petri dishes provided with a lid to prevent evaporation. After each determination, the fabric was transferred into a sterile 2 mL Eppendorf tube containing 1 mL autoclaved NaCl/KCl saline solution. This solution was subsequently mixed thoroughly using a Vortex for 3 min. Serial dilutions were made in NaCl/KCl solution. A 100 μL aliquot was pipetted onto a nutrient agar plate and then spread over the surface of the plate using standard plate method. Agar plates were incubated lid down, at 37 °C for 24 h before colonies were counted. Three independent assays were done for each sputtered sample during the course of this study. To verify that no re-growth of *E. coli* occurs after the first bacterial inactivation cycle, the TiO_2/Cu-film was incubated for 24 h at 37 °C. Then, the bacterial suspension of 100 μL was deposited on three Petri dishes to obtain replicates. The samples were incubated at 37 °C for 24 h. No bacterial re-growth was observed for these samples.

For MRSA testing, PES samples (4 cm^2) were inoculated with 20 μl of cell culture and incubated for 30, 60 and 120 min in a humidified chamber at room temperature (RT) in the dark or under light. The temperature inside the light box was maintained

(20–23 °C). Bacterial loss of viability on TiO_2/Cu-PES samples was then evaluated by direct agar transfer plate (incubated at 37 °C).

2.3.2. Irradiation sources

The irradiation of the *E. coli* and MRSA bacteria on the co-sputtered samples was carried by a Philips Master TLD-18 W/865 actinic lamps as used in hospital facilities with an emission between 400 and 720 nm with different light doses between 1.01 mW/cm^2 and 4.65 mW/cm^2.

3. Results and discussion

3.1. Surface characterization of sputtered TiO_2/Cu-PES

Co-sputtering Ti and Cu for 3 min in Ar-O_2 atmosphere led to a coating thickness of ~135 nm (equivalent to ~700 atomic layers). The Cu, TiO_2 and TiO_2/Cu content were determined by X-ray fluorescence (XRF) and are reported in Table 1. The amounts of Cu and TiO_2 are seen to increase with sputtering time as expected. It is important to note that TiO_2 sputtered for ~2 min has an equivalent to the amount of TiO_2 co-sputtering TiO_2/Cu for 3 min. CuO sputtered for ~1 min deposited Cu equivalent to a Cu/TiO_2 film co-sputtered for 3 min.

The diffuse reflectance spectra (DRS) show an increase in the optical absorption as a function of the co-sputtering time in Kubelka-Munk units up to 3 min as shown in Fig. 1. The wide spectral range for Cu(I)/Cu(II)-species between 200 and 800 nm extending allows a considerable absorption of the actinic light between 400 and 700. The optical absorption between 500 and 600 nm is due to the inter-band transition of Cu(I) and the absorption between 600 and 720 nm is attributed to the exciton band and the Cu(II) *d–d* transition fluorescence stereomicroscopy [17,21].

Fig. 2 shows the transmission electron microscopy (TEM) of TiO_2/Cu co-sputtered for 3 min on PES. The more dense Cu-clusters presented diameters between 16 and 20 nm while the TiO_2 clusters revealed smaller sizes between 5 and 10 nm. The TiO_2/Cu coating of 120–160 nm thick (500–800 atomic layers) presented a close contact between the TiO_2 and Cu-nanoparticles.

3.2. Evaluation of the E. coli reduction and effect of the applied light dose

Fig. 3 shows the bacterial reduction by TiO_2/Cu-PES under actinic light irradiation and in dark as a function of TiO_2/Cu co-sputtering times. PES by itself in the dark and actinic light does not reduce *E. coli*. But in the dark, *E. coli* bacterial reduction proceeds within 120 min in the dark on TiO_2/Cu-PES. The mechanism of TiO_2/Cu mediated *E. coli* inactivation under light irradiation has been reported in detail and for this reason it will not be addressed in the present study [13,14,16–18]. Reduction in the dark as shown in Fig. 3, trace 4 proceeds through a mechanism involving the

Table 1
Cu, TiO_2 and TiO_2/Cu determined by X-ray fluorescence (XRF) as a function of the DC-sputtering time.

Sample	%wt Cu/wt PES	%wt CuO/wt PES	%wt Ti/wt PES	%wt TiO_2/wt PES
Cu (5 min)	0.19	0.24	–	–
Cu (3 min)	0.16	0.20	–	–
Cu (1 min)	0.05	0.07	–	–
TiO_2 (5 min)	–	–	0.13	0.20
TiO_2 (3 min)	–	–	0.12	0.14
TiO_2 (1 min)	–	–	0.09	0.10
TiO_2/Cu (5 min)	0.09	011	011	0.17
TiO_2/Cu (3 min)	0.06	0.07	0.10	0.14
TiO_2/Cu (1 min)	0.02	0.04	0.02	0.03

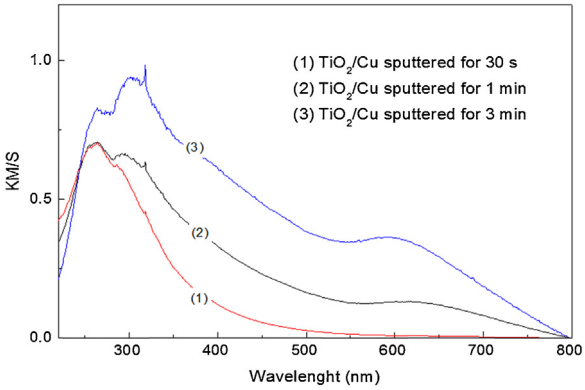

Fig. 1. Diffuse reflectance spectroscopy (DRS) of co-sputtered TiO_2/Cu on PES for the times: (1) 30 s, (2) 1 min and (3) 3 min.

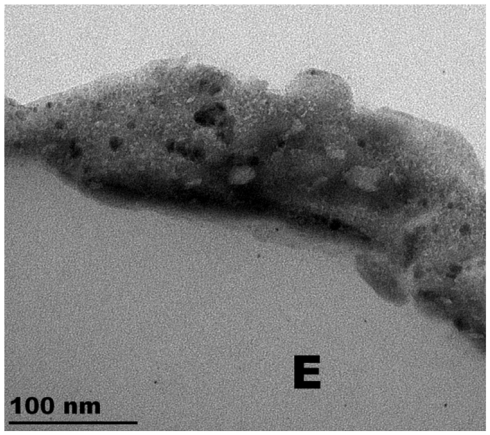

Fig. 2. Transmission electron microscopy (TEM) of TiO_2/Cu co-sputtered for 3 min on PES. E stands for the epoxide that is required to embed the sample during the preparation of the TEM image.

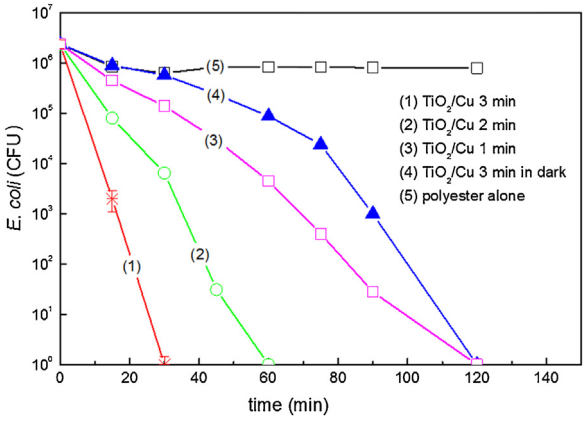

Fig. 3. *E. coli* inactivation on TiO_2/Cu co-sputtered for different times on PES as indicated in the traces: (1) 3 min, (2) 2 min, (3) 1 min, (4) co-sputtered TiO_2/Cu for 3 min in the dark and (5) PES-alone. The bacterial reduction under light irradiation used a lamp Philips Master-18 W/865 (4.65 mW/cm^2).

reaction of O_2 (air) with the Cu/Cu-ions. It will be discussed below in the XPS section and to suggest a possible reaction mechanism

Fig. 3, trace 1 shows a complete bacterial reduction under visible light irradiation within 30 min for TiO_2/Cu samples co-sputtered for 3 min. In this case, sufficient amount of TiO_2 and Cu was coated on the PES leading to a number of exposed catalytic sites inducing the fastest *E. coli* load reduction (see Table 1). Co-sputtering for 1 and 2 min (Fig. 3, traces 2 and 3) did not attain the necessary TiO_2 and

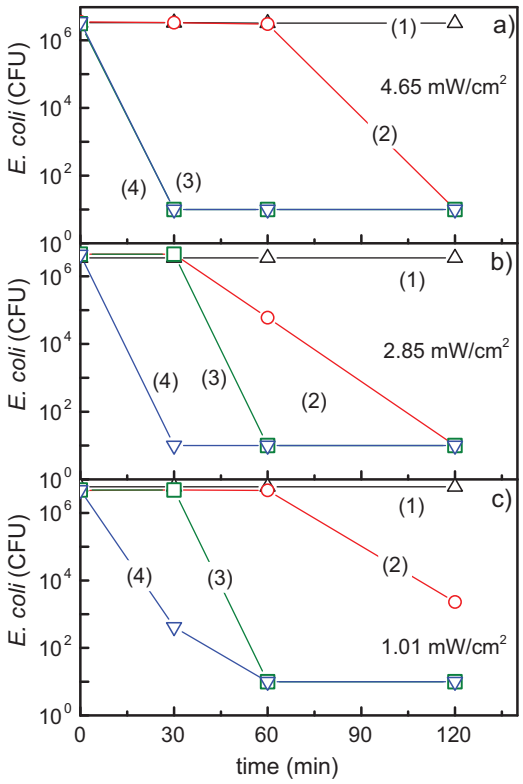

Fig. 4. *E. coli* reduction under Philips Master-18 W/865 (4.65 mW/cm^2) light irradiation: (1) PES alone (2) TiO_2 sputtered on PES for 2 min, (3) TiO_2/Cu-PES sputtered 3 min and (4) Cu sputtered on polyester for 1 min.

Cu sites to induce fast bactericidal activity. Fig. 3, trace 4 shows the complete bacterial reduction in the dark, a more important results than bacterial reduction induced by light due to the continuous nature of the dark bacterial reduction process. The effect of Cu on bacteria has been associated with the ingestion of copper leading to adverse reactions with transport-proteins of enzymes regulating the respiratory chain [16,17,23–26].

Fig. 4 show that TiO_2/Cu-PES surfaces damage the *E. coli* cell wall more than the TiO_2 surface under light and in the dark due to the added effect of cytotoxic Cu. This suggests that *E. coli* damage is located at the cell wall [27] in contact with the bactericide TiO_2/Cu-PES surface in Fig. 4. TiO_2 and Cu on PES proceeded with a similar trend in the bacterial reduction kinetics in Fig. 4. Increased Cu-loading on PES led to faster bacterial inactivation kinetics, but this effect was not observed in the case of TiO_2 (Fig. 4).

Fig. 4 also presents the effect of the actinic light intensity on the *E. coli* reduction mediated by TiO_2/Cu-PES surface at different light intensities. At the highest light dose of 4.65 mW/cm^2 the PES by itself does not lead to *E. coli* reduction (Fig. 4a, trace 1). TiO_2 sputtered samples for 2 min are seen to inactivate *E. coli* within 120 min (Fig. 4a, trace 2). Fig. 4a, trace 4 indicate that Cu sputtered for 1 min with the same surface content of Cu found in TiO_2/Cu co-sputtered for 3 min reduced *E. coli* as TiO_2/Cu-samples co-sputtered for 3 min. A similar trend was observed for the *E. coli* bacterial reduction applying intensities of 2.85 mW/cm^2 (Fig. 4b) and 1.01 mW/cm^2 (Fig. 4c). Under light irradiation TiO_2/Cu is a p-type semiconductor with band gap of 1.7 eV, a flat-band potential of −0.3 V vs SCE (pH 7) and a valence band of +1.4 V SCE [22].

Fig. 4a shows that the bacterial reduction effect shown by TiO_2 (trace 2) is far below the bacterial reduction induced by Cu (trace 4). TiO_2 is acting as a semiconductor generating highly oxidative species under light irradiation. But Cu induces toxicity in the sputtered films that more effectively inactivate bacteria. The interfacial charge transfer (IFCT) [17] from CuO to TiO_2 inhibits the O_2 reduction by Cu_2O/CuO since cb electrons are injected into the TiO_2 decreasing the amount of electrons available to reduce O_2 by Cu_2O/CuO that subsequently would lead more effectively to HO_2° and OH°.

The effect of the light dose in Fig. 4 shows that the density of active sites on the TiO_2/Cu-PES surface leading to *E. coli* reduction is higher than the photon/cm^2 reaching the TiO_2/Cu-PES surface. A higher light dose led to light saturation on the photocatalyst accelerating bacterial reduction (Fig. 4). Cu/CuO/NPs-ions and other heavy metals have been reported to denature bacteria proteins by binding to reactive groups resulting in their precipitation and inactivation through an oligodynamic effect [28,29]. This last effect will be accounted in the section below providing the data for the Cu released in ppb quantities during bacterial reduction as monitored by ICP-MS.

3.3. Repetitive bacterial reduction and Ti and Cu-release during disinfection: mechanistic implications

Repetitive bactericidal cycles of *E. coli* were carried out by TiO_2/Cu-PES under light irradiation and showed a stable repetitive performance (data not shown). The time necessary for the complete bacterial reduction up to the 5th cycle was about 40 min and increased by a small amount during the last repetitive recycling. After each cycle, the co-sputtered samples were washed thoroughly with sterilized MQ-water, vortexed for 3 min and dried. No bacteria remained on the TiO_2/Cu-PES sample. This observation moved us to assess by ICP-MS, the Cu- and Ti-release from the TiO_2/Cu-PES during bacterial reduction. The metal released during the bacterial reduction cycles when sputtering separately Ti (2 min) and Cu (1 min) on PES is shown in Table 2. Table 2 shows the Cu, Ti release at the end of the bacterial reduction when both metals were co-sputtered for 3 min. The release of Ti and Cu decreases to 2 and 4 ppb/cm^2, respectively after the fifth bacterial reduction cycle. Table 2 shows that the Cu and TiO_2 released during the cycles leading to complete reduction on samples co-sputtered for 3 min are significantly below the Cu and TiO_2 amounts released from samples loaded independently with similar amounts of Cu and TiO_2 on PES. A slower release of Cu allows a longer operational lifetime for the TiO_2/Cu-PES samples inducing bacterial reduction and this is important for any practical application of these films.

The copper toxicity toward mammalian cells have been reported with a median of lower effective concentration at 50% e.g. (L(E)C50 of 25 mg/L for mammalian cells [23–26]. The low release Cu of 4 < 25 ppb/cm^2 shown in Table 2 is well below the Cu-cytocompatible level [23]. Cu-levels of 4 ppb/cm^2 inducing bacterial reduction provide disinfection through an effective

Table 2
Metal-ions released during bacterial loss of viability cycles when sputtering TiO_2 or Cu on PES compared to ions release in co-sputtered TiO_2/Cu-PES.

		First cycle	Third cycle	Fifth cycle
TiO_2-PES (2 min)	Ti (ppb/cm^2)	14	11	8
Cu-PES (1 min)	Cu (ppb/cm^2)	11	5	9
Co-sputtered TiO_2/Cu-PES (3 min)	Ti (ppb/cm^2)	7	3	2
	Cu (ppb/cm^2)	6	4	4

Table 3
Surface atomic percentages determined by XPS of TiO_2/Cu-PES co-sputtered for 3 min as detected by XPS.

	C	O	N	Cu	Ti
Before bacterial loss of viability	31.8	22.1	0.7	19.3	26.1
After bacterial loss of viability	39.0	19.4	0.9	16.6	24.1

oligodynamic [17]. The Cu-ions have been reported to bind S, N and COO^- and other electron donor negative groups of the bacteria cell wall or entering the bacteria cytoplasm. Copper in the blood exists in two forms: bound to ceruloplasmin (85–95%), and the rest "free Cu" loosely bound to small molecules, protein, lipids and DNA.

The small amounts of toxic Cu NP's below 25 ppb/cm^2 released by the Cu-polyester allow for a higher cytocompatibility compared to a similar Ag-concentration as reported for mammalian cells. Cu is a metabolizable agent compared to Ag remaining in the body after ingestion increasing the Ag-serum levels [23–27].

3.4. Ar etching of TiO_2/Cu-PES film and Ti, Cu depth profile determined by XPS

By XPS the depth of Cu deposition on PES was investigated as well as the state of oxidation of the Ti- and Cu-species during bacterial reduction. The surface atomic percentage composition of C, O, N, Cu, and Ti is shown in Table 3 at time zero and after 30 min bacterial reduction of *E. coli* as shown in Fig. 3, trace 1. Table 3 shows a small increase in the C-content due to bacterial decomposition residues besides the C-absorbed from the atmosphere during the bacterial reduction. A small decrease in the Cu and Ti-surface concentration after 30 min bacterial reduction was observed and was triggered by the increase of C on the topmost layers described in the preceding paragraph.

Fig. 5a presents the Cu doublet at time zero and Fig. 5b presents the changes in the XPS spectra after bacterial reduction. This doublet is attributed to the presence of the Cu^{2+}-oxidation state (Cu^{2+}) prevalent in the Cu-sputtered sample exposed to air [13,16]. The Cu/Cu_2O with BE 932.2 eV at time zero remains stable after bacteria reduction at 933.1 eV. The CuO deconvoluted peak at time zero shifts to 943.2 eV after bacterial reduction as shown in Fig. 5b. A shift of >0.2 eV is indicative of a change in the oxidation state in the XPS specie [20,21]. Redox catalysis seems to take place during the disinfection process. The redox chemistry is associated with the production of highly oxidative radicals for composites of TiO_2 and Cu-composites [13–15].

The Cu oxidation state at time zero was monitored to be 75.5% for Cu/Cu_2O and 24.3% for CuO. A significant change in the oxidation state was observed after bacterial reduction rendering Cu/Cu_2O 14.1% and 85.7% for CuO. The Ti^{3+}/Ti^{4+} surface electron traps have been reported to enhance the O_2 chemisorption in the presence of Cu in TiO_2/Cu-more markedly than in the case of TiO_2 alone [17].

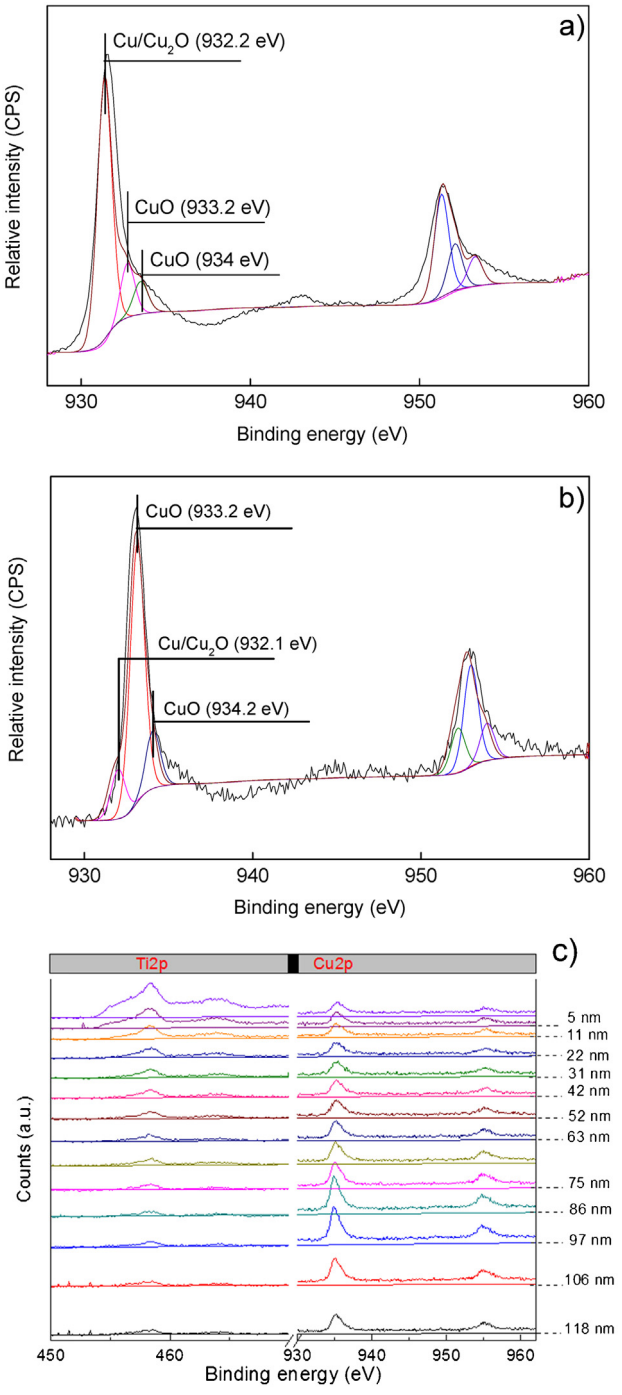

Fig. 5. (a) XPS deconvolution of the Cu2p peak of co-sputtered TiO_2/Cu PES 3 min samples (a) before bacterial reduction of *E. coli*. (b) XPS deconvolution of the Cu2p peak of co-sputtered TiO_2/Cu PES 3 min samples bacterial inactivation of *E. coli* under a Philips Master lamp irradiation18 W/865 (4.65 mW/cm^2). (c) XPS of the TiO_2/Cu-PES top-most layers for a sample co-sputtered for 3 min and etched by Ar^+-ions (5 keV) up to a depth of 118 nm.

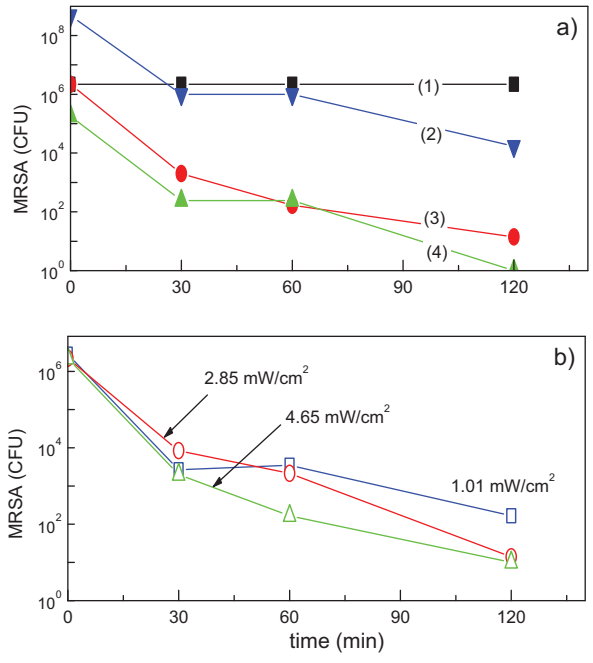

Fig. 6. (a) Effect of initial bacterial concentration of MRSA loss of viability on: (1) PES alone (2) co-sputtered TiO_2/Cu-PES for 3 min tested in the dark, 10^8 CFU/ml, (3) co-sputtered TiO_2/Cu-PES for 3 min tested in the dark, 10^6 CFU/ml, (4) co-sputtered TiO_2/Cu-PES for 3 min tested in the dark, 10^5 CFU/ml. (b) Effect of light intensity irradiation on MRSA bacterial reduction on co-sputtered TiO_2/Cu-PES for 3 min under: 1.01 mW/cm^2, 2.85 mW/cm^2 and 4.65 mW/cm^2.

Production of reactive oxygen species (ROS) by the Cu-clusters on the PES leads to bacterial inactivation due to the interaction of the Cu-clusters with *E. coli* in the dark

$$Cu^{+} + O_2{}^{\circ}- \leftrightarrow Cu^{\circ} + O_2 \quad (1)$$

$$Cu^{\circ} + O_2 \leftrightarrow Cu^{+} + O_2 \quad (2)$$

The CuO (Cu^{2+}) is reduced

$$Cu^{2+} + e^{-}_{cb} \leftrightarrow Cu^{+} \quad (3)$$

Or by a two electron transfer from Cu^{2+} leading to Cu° atoms

$$Cu^{2+} + 2e^{-} \leftrightarrow Cu^{\circ} \quad (4)$$

The Cu-atoms then coalesce to Cu° nanoparticles settling in the Cu-network of the PES with $E_{redox} = -0.34$ V vs. NHE [30].

Fig. 5c presents the deconvolution of the Ti and Cu, of TiO_2/Cu-PES samples co-sputtered for 3 min as a function of penetration depth of the Ar-ions. By following the decrease of the Ti2p doublet in Fig. 5 it is readily seen that the Ti penetration into the PES reaches ~118 nm (or ~600 atomic layers). The penetration depth of Cu in Fig. 5 on PES goes beyond 118 nm, since the Cu2p doublet is still present when the etching by Ar-ions has attained 118 nm. The etching of TiO_2/Cu-PES layers essentially takes off mostly the PES C-layers.

3.5. MRSA reduction as a function of initial CFU concentration and the effect of applied light intensity

Fig. 6a shows the MRSA reduction as a function of the bacterial loading of the sample on: (1) PES alone (2) co-sputtered TiO_2/Cu-PES for 3 min in the dark with 10^8 CFU/ml, (3) co-sputtered TiO_2/Cu-PES for 3 min in the dark with 10^6 CFU/ml, (4) co-sputtered TiO_2/Cu-PES for 3 min in the dark with 10^5 CFU/ml. After initial optimization the co-sputtered TiO_2/Cu-PES (3 min) samples presented an MRSA bacterial reduction above the activity presented by co-sputtered TiO_2/Cu-PES samples sputtered for 1 and 2 min and are therefore the results presented in Fig. 6. The bacterial reduction of MRSA in the dark is an important observation indicating the potential use of this catalyst in health facilities without any necessity of using photo-energy to activate the disinfection process.

Fig. 6b shows the effect of light intensity on MRSA bacterial reduction by a TiO_2/Cu-PES sample co-sputtered for 3 min applying light intensities of 1.01 mW/cm^2, 2.85 mW/cm^2 and 4.65 mW/cm^2. Fig. 6b shows that only a marginal increase in the MRSA bacterial

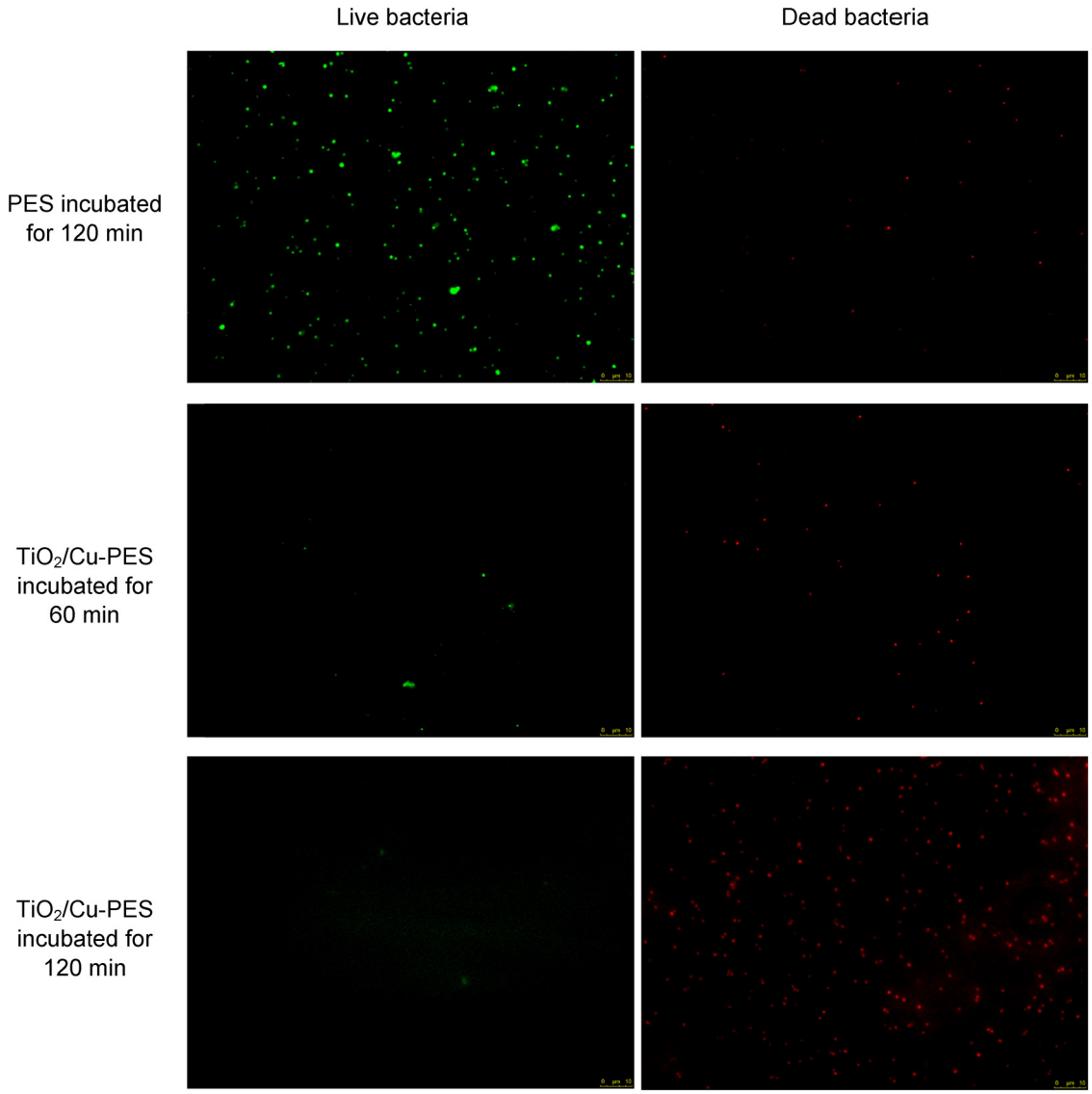

Fig. 7. Stereomicroscopy images of live and dead *E. coli* on TiO_2/Cu-PES showing the loss of bacterial viability within 120 min.

reduction was observed with an increase in light intensity. We suggest that the MRSA reduction is predominantly controlled by the Cu/Cu-ions inherent toxicity and not by the reactive oxygen species (ROS) induced by light irradiation of the TiO_2/Cu-PES sample.

In the case of *E. coli* bacterial reduction under light shown in Fig. 4a, the TiO_2/Cu-PES samples sputtered for 3 min (trace 3) reduced by a factor of two the *E. coli* reduction time when the light intensity was increased from 1.01 to 4.65 mW/cm^2. An accelerated reduction was observed for *E. coli*, but this was not the case for MRSA. The Gram-negative *E. coli* has a thinner peptoglycan cell wall compared to the Gram-positive MRSA and containing additional bilayers with a high structural complexity [11,12]. The significant difference in wall thickness/wall microstructure between MRSA and *E. coli* lead to the different interaction for *E. coli* and MRSA with TiO_2/Cu-PES surface under light irradiation. MRSA is a Gram-positive bacteria presenting a cell-wall ~40–80 nm thick with a peptoglycan content >50%, a lipid content of <3% and no lipo-polysaccharide content. *E. coli* is a Gram-negative bacteria presenting a cell wall thickness of ~10 nm with a peptoglycan content of 10–20%, a lipid content of <58% and a lipo-polysaccharide content of 13%.

Kühn et al. [31] reported recently a fast bacterial reduction of *E. coli* and *P. aeruginosa* compared to *Staphyloccocus aureus* presenting a thicker cell wall. Another important difference for the interaction of both types of bacteria with CuNP's is the strong electrostatic interaction of Cu NP's-positive-ions with the negative lipopolysaccharide (LPS) outer layer of *E. coli*. This is not the case for the interaction between MRSA and the Cu NP's positive-ions since both surfaces present similar charges. Cu-NP's absorption has been reported on the teichoic acid and the peptoglycan outer MRSA cell wall [32]. For *E. coli* and MRSA the bacterial reduction has been reported to occur on several metal and oxide agents [29,33,34].

3.6. E. coli *staining and viability on TiO_2/Cu-PES samples*

Fig. 7 shows the live and dead *E. coli* bacteria by using the dye fluorochrome that enters the cell and stains the DNA only if the cell wall membranes are damaged since under this condition they show an abnormal high permeability [35]. To test the time at which *E. coli* cells suffer destabilization/damage of the cell wall leading ultimately to cell dead (red dots indicate membrane damage), the cells were incubated on PES in the dark and also incubated for 60 and 120 min on TiO_2/Cu-PES. The *E. coli* cells kept alive (green dots) on PES alone up to 120 min of incubation. But for cell incubated for 60 and 120 min on TiO_2/Cu-PES, the loss of viability becomes faster as the incubation time increases leading to membrane damage and cell death as shown by the red dots in Fig. 7 [36].

4. Conclusions

The trend presented in visible light induced bacterial extent and reduction kinetics of *E. coli* and MRSA on TiO_2/Cu-PES are shown to be different. Possible reasons are suggested/discussed to account this observation. There seems to be a significant stabilizing effect of the TiO_2/Cu-PES on the release of Cu during bacterial reduction compared to Cu alone as monitored by ICP-MS in the ppb range. This suggests an oligodynamic effect responsible for the bacterial reduction of *E. coli* and MRSA. This effect is beneficial for a longer operational lifetime during repetitive bacterial reduction processes.

Acknowledgements

We thank the EPFL, Swiss National Science Foundation (SNF) Project (200021-143283/1) and the EC7th Limpid FP project (Grant No. 3101177) "Photocatalytic materials for depollution" for their financial support. We also thank the CIME-EPFL for microscopy experiments, the COST Actions MP1101 and MP1106 for interactive discussions during the course of this study.

References

[1] W.H. Boucher, G.H. Talbot, J.S. Bradley, J.S. Edwards, D. Gilbert, L.B. Rice, M. Scheld, B. Spellberg, J. Bartlett, Clin. Infect. Dis. 48 (2009) 1–12.
[2] D. Pittet, D. Tarara, P.R. Wenzel, J. Am. Med. Assoc. 271 (1994) 1598–1601.
[3] B. Allegranzi, S. Bagheri-Nejad, C. Combescure, W. Graafmans, H. Attar, L. Donaldson, D. Pittet, Lancet 377 (2011) 228–241.
[4] R. Plowman, N. Graves, A. Griffin, L.A. Roberts, V. Swan, B. Cookson, Taylor, J. Hosp. Infect. 47 (2001) 198–204.
[5] S. Dance, J. Hosp. Infect. 7 (2007) 378–389.
[6] I. Kramer, I. Schwebke, G. Kampf, BMC Infect. Dis. 6 (2006) 137–146.
[7] A. Mills, P. Hill, P. Robertson, J. Photochem. Photobiol. A 237 (2012) 7–23.
[8] K. Page, W. Wilson, I.P. Parkin, J. Mater. Chem. 19 (2009) 3819–3831.
[9] M.S.P. Dunlop, C. Sheeran, J.-A. Byrne, A. McMahon, S. Boyle, M.A.S. McGuigan, J. Photochem. Photobiol. A 216 (2010) 303–3010.
[10] H. Ishiguro, Y. Yao, Y. Nakano, M. Hara, K. Sunada, K. Hashimoto, J. Kajioka, S. Fujishima, Y. Kubota, Appl. Catal. B 129 (2013) 56–61.
[11] H. Foster, I. Ditta, S. Varghese, A. Steele, Appl. Microbiol. Biotechnol. 90 (2010) 1847–1868.
[12] M. Pelaez, N. Nolan, S. Pillai, M. Seery, P. Falaras, A. Kontos, M.S.P. Dunlop, J. Hamilton, J.-A. Byrne, K. O'Shea, M. Enterazi, D. Dionysiou, Appl. Catal. B 25 (2012) 331–349.
[13] X. Qiu, M. Miyauchi, K. Sunada, M. Minoshima, M. Liu, Y. Lu, L. Ding, Y. Shomodaira, Y. Hosogi, Y. Kuroda, K. Hashimoto, ACS Nano 6 (2012) 1609–1618.
[14] K. Sunada, S. Watanabe, K. Hashimoto, Environ. Sci. Technol. 40 (2003) 4785–4789.
[15] L. Zhang, R. Dillert, D. Bahnemann, M. Vormoor, Energy Environ. Sci. 5 (2012) 7491–7507.
[16] S. Rtimi, O. Baghriche, C. Pulgarin, R. Sanjines, J. Kiwi, ACS Appl. Mater. Interfaces 4 (2012) 5234–5240.
[17] S. Rtimi, O. Baghriche, C. Pulgarin, J.-C. Lavanchy, J. Kiwi, Surf. Coat. Technol. 232 (2013) 804–813 (and references therein).
[18] L. Rio, E. Kusiak, J. Kiwi, C. Pulgarin, A. Trampuz, A. Bizzini, J. Appl. Microbiol. 78 (2012) 8176–8182.
[19] G. Borkow, J. Gabbay, Curr. Chem. Biol. 3 (2009) 272–278.
[20] C. Wagner, W. Riggs, L. Davis, G. Mullenberg (Eds.), Handbook of X-ray Photoelectron Spectroscopy, Perkin-Elmer Corporation Physical Electronics Division, Minnesota, USA, 1979.
[21] J. Nogier, M. Delamar, P. Ruiz, M. Gratzel, R. Thampi, J. Kiwi, Catal. Today 20 (1994) 109–123.
[22] K. Hardee, A. Bard, J. Electrochem. Soc. 124 (1977) 215–224.
[23] O. Bondarenko, J. Katre, Archiv. Toxicol. 87 (2013) 1181–1200.
[24] http://www.opsi.gov.uk/si/si2000/20003184.htm#30
[25] F. Heidenau, W. Mittelmeier, R. Detsch, F. Haenle, G. Stenzel Ziegler, G. Gollwitzer, J. Mater. Sci. Med. 16 (2005) 883–889.
[26] J. Brewer, J. Clinic. Neurophys. 121 (2010) 459–460.
[27] S. Rtimi, R. Sanjines, M. Andrzejczuk, C. Pulgarin, A. Kulik, J. Kiwi, Surf. Coat. Technol. 254 (2014) 333–343 (and references therein).
[28] W.K. Nägeli, Denkschr. Allgemein. Naturfors. Ges. (English archive) 33 (1983) 174–182.
[29] E. Rentz, J. Nutr. Environ. Med. 13 (2003) 109–118.
[30] M. Pourbaix, Atlas of Electrochemical Equilibria in Aqueous Solutions, Nace International Pub. Co., Cebelcor, Brussels, 1974.
[31] K. Kühn, I. Chaberny, K. Massholder, M. Sticker, V. Benz, H.-G. Sonntag, I. Erdinger, Chemosphere 53 (2003) 71–77.
[32] C. Espirito Santo, E. Lam, C. Elowsky, D. Quarnta, D. Domaille, C. Chang, G. Grass, Appl. Micro. Environ. 77 (2011) 794–802.
[33] A. Thill, O. Zeyons, O. Spalal, F. Chauvat, J. Rose, M. Auffan, A.-M. Flank, Environ. Sci. Technol. 40 (2006) 6151–6156.
[34] V. Nadtochenko, A. Rincon, S. Stanka, J. Kiwi, J. Photochem. Photobiol. A 169 (2005) 131–137.
[35] C. Gunawan, W. Teoh, C. Marquis, R. Amal, Small 9 (2013) 3554–3560.
[36] I. Vizcarra, Ph. Emge, Ph. Miermeister, M. Chabria, R. Konradi, V. Vogel, J. Möller, Biointerphases 8 (2013) 22–30.